Published in final edited form as:

Nature. 2018 January 18; 553(7688): 291–294. doi:10.1038/nature25178.

Dietary trehalose enhances virulence of epidemic *Clostridium difficile*

J. Collins[1], **C. Robinson**[2], **H. Danhof**[1], **C.W. Knetsch**[3], **H.C. van Leeuwen**[3], **T.D. Lawley**[4], **J.M. Auchtung**[1], and **R.A. Britton.**[1,*]

[1]Baylor College of Medicine, Department of Molecular Virology and Microbiology [2]University of Oregon, Institute for Molecular Biology [3]Leiden University Medical Centre, Department of Medical Microbiology, The Netherlands [4]Wellcome Trust Sanger Institute, Wellcome Trust Genome Campus, United Kingdom

Abstract

Clostridium difficile disease has recently increased to become a dominant nosocomial pathogen in North America and Europe, although little is known about what has driven this emergence. Here we show two epidemic ribotypes (RT027 and RT078) have acquired unique mechanisms to metabolize low concentrations of the disaccharide trehalose. RT027 strains contain a single point mutation in the trehalose repressor that increases this ribotype's sensitivity to trehalose by >500 fold. Furthermore, dietary trehalose increases virulence of a RT027 strain in a mouse model of infection. RT078 strains acquired a cluster of four genes involved in trehalose metabolism, including a PTS permease that is both necessary and sufficient for growth on low concentrations of trehalose. We propose that the implementation of trehalose as a food additive into the human diet, shortly before the emergence of these two epidemic lineages, helped select for their emergence and contributed to hypervirulence.

Whole genome sequencing analysis of *C. difficile* ribotype 027 (RT027) strains demonstrated that two independent lineages emerged in North America from 2000-2003.[1] Comparison with historic, pre-epidemic, RT027 strains showed that both epidemic lineages acquired a mutation in the *gyrA* gene, leading to increased resistance to fluoroquinolone antibiotics. While the development of fluoroquinolone resistance (FQR) has almost certainly

*Correspondence to: Robert.Britton@bcm.edu.

Data availability statement

The data that support the findings of this study are available from the corresponding author upon reasonable request. Source data for figures [1-5 and Extended Data 2, 3, and 5] are provided with the paper.

Author Contributions Concept and design of study RAB, JMA, JC, CR. Experiments: *C. difficile* growth, JC & CR; identification of L172I SNP and comparative analysis, CR & JC; *treA* RT-qPCR, HD; Mouse infection model, JC; Genetic manipulation of *C. difficile* strains, JC and CR; identification of RT078 trehalose insertion, CWK, HCL, TDL; Faecal minibioreactor competitions, JMA; Spontaneous *C. difficile* mutant identification, HD; Analysis by JC, CR, HD, JMA, and RB; manuscript drafted by JC, JMA, RAB; Critical manuscript revision by all authors.

The authors declare no competing financial interests.

played a role in the spread of RT027 strains, FQR has also been observed in non-epidemic *C. difficile* ribotypes and identified in strains dating back to the mid-1980s.[2,3] Thus, other factors likely contributed to the emergence of epidemic RT027 strains.

The prevalence of a second *C. difficile* ribotype, RT078, increased 10-fold in hospitals and clinics from 1995-2007 and was associated with increased disease severity.[4] However, the mechanisms responsible for increased virulence remain unknown.[5–8] It is noteworthy that RT027 and RT078 lineages are phylogenetically distant from one another (Extended Data Fig. 1), indicating that the evolutionary changes leading to concurrent increases in epidemics and disease severity might have emerged by independent mechanisms.[9]

Epidemic RT027 and RT078 strains can grow on low concentrations of trehalose

Ribotype 027 strains exhibit a competitive advantage over non-RT027 strains *in vitro* and in mouse models of CDI.[10] To investigate potential mechanisms for increased fitness, we examined carbon source utilization in an epidemic RT027 isolate (CD2015) using the Biolog 96-well Phenotype MicroArray carbon source plates (see Methods and Extended Data Table 1). Out of several carbon sources identified that supported CD2015 growth, we found the disaccharide trehalose increased the growth yield of CD2015 by approximately 5-fold compared to a non-RT027 strain. To examine the specificity of enhanced growth on trehalose across *C. difficile* lineages, 21 strains encompassing 9 ribotypes were grown on a defined minimal medium (DMM) supplemented with glucose or trehalose as the sole carbon source. All *C. difficile* strains grew robustly with 20 mM glucose, however, only epidemic RT027 (n=8) and RT078 (n=3) strains exhibited enhanced growth on an equivalent trehalose concentration (10 mM; Fig. 1). Increasing the trehalose concentration to 50 mM enabled growth in most ribotypes (Extended Data Fig. 2a).

Molecular basis for RT027 growth on low levels of trehalose

To identify the genetic basis for enhanced trehalose metabolism, we compared multiple *C. difficile* genomes. All *C. difficile* genomes encode a putative phosphotrehalase enzyme (*treA*) preceded by a transcriptional repressor (*treR*) (Fig. 2a). Phosphotrehalase enzymes metabolize trehalose-6-phosphate into glucose and glucose-6-phosphate. To test whether *treA* was essential for trehalose metabolism, we generated *treA* deletion mutants in the RT027 strain R20291 (R20291Δ*treA*) and the RT012 strain CD630 (CD630Δ*treA*) and grew them in DMM supplemented with 50 mM trehalose. The lack of *treA* prevented growth in both knockout strains that could be complemented by plasmid expression of *treA* (Extended Data Fig. 2b). Thus, *treA* is required to metabolize trehalose.

We next asked if RT027 strains have altered regulation of the *treA* gene when compared to other ribotypes. To test this hypothesis and determine the minimum level of trehalose required to activate *treA* expression, we grew CD2015 (RT027) and CD2048 (RT053) and exposed them to increasing amounts of trehalose. We found that the RT027 strain turned on *treA* expression at 50 μM trehalose, a concentration 500-fold lower than that required to turn on *treA* in RT053 (Fig. 2b). To confirm this phenotype, we took four RT027 strains and four

non-RT027 strains and measured expression of *treA* in a single trehalose concentration. Again, RT027 strains exhibited significantly higher *treA* expression than all other ribotypes (P=0.029, Extended Data Fig. 3). These results support the idea that RT027 strains are exquisitely sensitive to low concentrations of trehalose.

Sequence alignment of the trehalose operon across 1,010 sequenced *C. difficile* strains revealed a conserved single nucleotide polymorphism (SNP) within the *treR* gene of all RT027 strains ($TreR_{RT027}$) (Extended Data Fig. 4a). The SNP encodes an L172I amino acid substitution near the predicted effector (trehalose-6-phosphate) binding pocket of TreR (Fig. 2c), a site that is highly conserved across multiple species (93.9% conservation, Extended Data Fig. 4b). This SNP is found not only in every RT027 strain sequenced to date, but is also present in a newly isolated fluoroquinolone sensitive ribotype (RT244) that has caused community-acquired epidemic outbreaks in Australia[11,12] and other ribotypes very closely related to RT027, such as RT176 which has caused epidemic outbreaks in the Czech Republic and Poland.[13,14] Like RT027 strains, the RT244 strains DL3110 and DL3111 can grow on 10 mM trehalose (Extended Data Fig. 2c).

To determine the types of spontaneous mutations that lead to enhanced trehalose utilization, we cultivated several non-RT027/RT078 strains under low trehalose concentrations in minibioreactors.[10] After 3 days of continuous cultivation, 13 independent spontaneous mutants capable of growing on low concentrations (< 10 mM) of trehalose were isolated. All thirteen mutants contained either nonsense or missense mutations in the *treR* gene (Extended Data Table 2).

Impact of trehalose metabolism on disease severity

To test whether the ability of *C. difficile* RT027 strains to metabolize trehalose impacts disease severity, we performed two different experiments. In the first, humanized microbiota mice were challenged with 10^4 spores of either R20291 (RT027, n=27) or R20291Δ*treA* (n=28). Following infection, trehalose (5 mM) was provided *ad libitum* in the drinking water and disease progression monitored. The R20291Δ*treA* mutant demonstrated a dramatic decrease in mortality (33.3 vs 78.6%) when compared to R20291 (78% lower risk with R20291Δ*treA*; hazard ratio, 0.22; 95% CI, 0.09 to 0.59; P=0.003, likelihood ratio test P=0.002 (Fig. 3a). In the second experiment, we infected two groups of humanized microbiota mice with RT027 strain R20291. One group received 5 mM trehalose in water as well as a daily gavage of 300 mM trehalose (n=28) to mimic a dose expected in a meal for humans, whereas the control group (n=27) received a water control. Trehalose addition was found to cause increased mortality compared to the RT027 infected mice without dietary trehalose (3-fold increased risk with trehalose; hazard ratio, 3.20; 95% CI, 1.09 to 9.42; P=0.035, likelihood ratio test P=0.026, Fig 3b). Combined, these results show that metabolism of dietary trehalose can contribute to disease severity of RT027 *C. difficile* strains.

To identify the cause of increased disease severity when trehalose is present, we challenged mice with either R20291 or R20291Δ*treA* and provided 5 mM trehalose *ad libitum* in the drinking water. Forty-eight hours post challenge, *C. difficile* load and toxin levels were

measured. Over two independent experiments, no significant difference in *C. difficile* numbers were observed, however, a significant increase in relative toxin B levels was detected (median 9.2 X10^4, IQR 5.1 × 10^4−1.0 × 10^5 Vs median 4.1 × 10^4, IQR 2.3 × 10^4−4.6 × 10^4, p=.0268, Extended Data Fig. 5). This increased toxin production could contribute to increased disease severity.

Molecular basis for RT078 growth on low levels of trehalose

Molecular basis for RT078 Unlike RT027, RT078 strains do not possess the TreR L172I substitution or other conserved SNPs in the *treRA* operon. To identify sequences of potential relevance to trehalose metabolism, we performed whole genome comparisons. A four-gene insertion was found in all RT078 strains sequenced to date, annotated to encode a second copy of a phosphotrehalase (TreA2, sharing 55% amino acid identity with TreA), a potential trehalose specific PTS system IIBC component transporter (PtsT), a trehalase family protein that is a putative glycan debranching enzyme (TreX), and a second copy of a TreR repressor protein (TreR2, sharing 44% amino acid identity with TreR) (see Fig. 4a). Genomic comparison of publicly available *C. difficile* genomes revealed the four-gene insertion was present in RT078 and the closely related RT033, RT045, RT066, and RT126 ribotypes and absent from reference genomes of any other *C. difficile* lineage (Extended Data Fig. 6).

To test whether the newly acquired transporter (*ptsT*) was responsible for enhanced trehalose metabolism, a *ptsT* deletion mutant was constructed in a RT078 (CD1015) strain. This strain was unable to grow on DMM supplemented with 10 mM trehalose (Fig. 4b), but retained the ability to grow in medium supplemented with 50 mM trehalose (Extended Data Fig. 2d). The growth defect in this deletion mutant (CD1015Δ*ptsT*) was directly due to the lack of *ptsT* since expression of *ptsT* from an inducible promoter could complement growth on 10 mM trehalose (Fig 4b).

We next tested if *ptsT* was sufficient to confer enhanced trehalose utilization in a non-ribotype 078 strain, which fails to grow under low trehalose concentrations. To this end, *ptsT* was expressed from an inducible promoter in strain CD630 (RT012). Expression of *ptsT* was sufficient to allow growth of CD630 in DMM supplemented with 10 mM trehalose (Fig. 4c). Taken together, we conclude that *ptsT* is both necessary and sufficient to support growth on low concentrations of trehalose.

To test whether the expression of *ptsT* could confer a fitness advantage, CD1015 (RT078) was competed against its isogenic CD1015Δ*ptsT* mutant in a human faecal minibioreactor (MBRA) model of CDI.[10] Following clindamycin treatment of MBRA communities to enable infection, CD1015 and CD1015Δ*ptsT* strains were added together to each reactor and levels monitored over time. Remarkably, the CD1015 strain was found to be significantly more efficient at competing *in vivo* in the presence of a complex microbiota than the CD1015Δ*ptsT* mutant (mean competitive index of 246 on day 7). To ensure the CD1015Δ*ptsT* loss was due to the absence of *ptsT*, CD1015 was competed against the CD1015Δ*ptsT* mutant complemented with *ptsT* from an inducible vector. After 5 days continuous competition, the wild-type RT078 had a mean competitive index of just 3.7 (Fig. 4d). Hence, *ptsT* provides a competitive fitness advantage to RT078 strains.

Significant amounts of dietary trehalose are observed in the distal gut

Despite the presence of a localized brush border trehalase enzyme in the small intestine, human studies suggest that high levels of trehalose consumption can result in significant amounts reaching the distal ileum and colon.[15–17] To demonstrate that a significant amount of dietary trehalose can survive transit through the small intestine, we gavaged mice with 100 μl (300 mM) trehalose (equivalent to the suggested concentration in ice cream) and measured trehalose levels in the cecum over time. Using clinical *C. difficile* strains as biosensors, we found the level of trehalose to be sufficient to activated *treA* gene expression in the RT027 strain CD2015 but not in RT053 strain CD2048 (Fig 5a). To test whether we could detect a low dietary amount of trehalose, we gavaged antibiotic treated mice with 100 μl (5 mM) trehalose and measured *treA* activation in these same strains. Again, the RT027 strain showed significant *treA* activation (Fig. 5b). Finally, to determine if trehalose is bioavailable in humans at sufficient levels to be utilized by epidemic *C. difficile* isolates, we tested ileostomy effluent from three anonymous donors consuming their normal diets. In 2 of 3 samples, *treA* expression was strongly induced in the RT027 strain CD2015 but not in the RT053 strain CD2048 (Fig. 5c), supporting the notion that levels of trehalose found in food is sufficient to be utilized by epidemic *C. difficile* strains.

Discussion

Containing an α,α-1,1-glucoside bond between two α-glucose units, trehalose is a non-reducing and extremely stable sugar, resistant to both high temperatures and acid hydrolysis. Although considered an ideal sugar for use in the food industry, the use of trehalose in the US and Europe was limited prior to 2000 due to high cost of production (~\$700 Kg^{-1}). The innovation of a novel enzymatic method for low cost production from starch made it commercially viable as a food supplement (~\$3 Kg^{-1}).[18] Granted GRAS (Generally Recognized As Safe) status by the FDA in 2000 and approved for use in food in Europe in 2001, reported expected usage ranges from concentrations of 2%-11.25% for foods including pasta, ground beef, and ice cream. The widespread adoption and use of trehalose in the diet coincides with the emergence of both RT027 and RT078 outbreaks (Fig. 6).

Several lines of evidence support that dietary trehalose has participated in the spread of epidemic *C. difficile* ribotypes. First, the ability of RT027 and RT078 strains to metabolize trehalose was present prior to epidemic outbreaks. The earliest retrospectively recorded RT027 isolate was the non-epidemic strain CD196, isolated in 1985 in a Paris hospital.[19] Three years later in 1988, another non-epidemic strain RT027 (BI1) was isolated in Minneapolis, Minnesota. Both isolates, in addition to every RT027 strain sequenced to date, contain the L172I substitution in TreR. RT078 strains were also present in humans prior to 2001, but epidemic outbreaks were not reported until 2003.[4] Second, RT027 and RT078 lineages are phylogenetically distant clades of *C. difficile*, yet have convergently evolved distinct mechanisms to metabolize low levels of trehalose. Third, increased disease severity of a RT027 strain that can metabolize trehalose in our CDI mouse model is consistent with increased virulence of RT027 and RT078 ribotypes observed in patients. Fourth, the ability to metabolize trehalose at lower concentrations confers a competitive growth advantage in the presence of a complex intestinal community. Finally, levels of trehalose in ileostomy

fluid from patients eating a normal diet are sufficiently high to be detected by RT027 strains. Based on these observations, we propose the widespread adoption and use of the disaccharide trehalose in the human diet has played a significant role in the emergence of these epidemic and hypervirulent strains.[20]

Methods

Bacterial strains and growth

A full list of strains can be found in Extended Data Table 3. Carbon source utilization of CD630 (RT012) and CD2015 (clinical RT027) was carried out using Biolog Phenotypic Microarray plates. Growth studies were carried out under anaerobic conditions (5% hydrogen, 90% nitrogen, 5% carbon dioxide). Strains were cultured in overnight in BHI media (Difco) supplemented with 0.5% w/v yeast extract. Growth assays utilized a defined minimal medium (DMM) as described previously[21] supplemented with either trehalose or glucose as indicated. Anhydrous tetracycline was used at 500 ng/ml to induce expression of *ptsT* or *treA* from ectopic expression vectors.

Comparative genomics

To identify unique functional features in RT078 strains, we reviewed publicly available *C. difficile* genomes covering all phylogenetic lineages[9] using a tool based on BLASTX comparisons of protein annotations.[22] The genomes included in the analysis were PCR RT012 (strain 630, lineage I), RT027 (R20291, lineage II), PCR RT017 (CF5, M68 lineage IV), and RT078 (QCD-23m63, CDM120 lineage V).

Genetic manipulation of *C. difficile*

Inactivation of *treA* in CD630 was accomplished by group-II intron directed insertion as previously described.[23] Primers were designed to target intron to insert at bp 177 of *treA* of CD630 (IBS1.2, EBS1, and EBS2; All primers are described in Extended Data Table 3). The resulting *treA* insertion-deletion mutant was verified by PCR using primer pair (CR064-CR065) designed to flank the *treA* insertion site, resulting in a 350bp product for the wild-type gene and a 2.4 kbp product for the gene knockout.

Clean deletions in R20291 and CD1015 were performed using a *pyrE* allelic exchange system as described previously.[24] This is the first case of the *pyrE* allelic exchange system being used in the RT078 lineage and required generation of CD1015Δ*pyrE* prior to further deletions. Complementation of *treA* and *ptsT* was carried out using an anhydrous tetracycline inducible system as described previously.[25] All plasmid conjugations into *C. difficile* strains were carried out with *E. coli* SD46. Cloning was accomplished with a combination of restriction digest and ligase cycling reactions as described previously.[26] Primers and detailed plasmid maps for construction of knockout strains are available at the links provided in Extended Data Table 3.

Quantitative real-time PCR with reverse transcription

Strains were grown overnight and subcultured 1:50 into DMM supplemented with 20 mM succinate. Upon reaching an OD_{600} of 0.2-0.3, indicated concentrations of trehalose were

added to the culture. After 30 minutes incubation, *C. difficile* cells were collected by centrifugation, resuspended in RNALater solution (Invitrogen), and stored at −80°C. Cells were resuspended in 1 ml RLT buffer (Qiagen RNeasy Kit) and lysed by bead beating (2 × 1 min) at 4°C followed by RNA extraction per manufacturers' instruction. cDNA was synthesized using Invitrogen Superscript III reverse transcriptase following the recommended protocol. Quantitative PCR reactions were performed in triplicate using Power SYBR Green PCR Master Mix (ABI) with either *C. difficile* 16s (JP048-JP049) or *treA* (CR045-CR046) specific primers. Standard curves of cDNA were run to determine primer efficiencies and calculated as per Pfaffl et al.[27] Expression of *treA* was determined using an average of triplicate C_T values from each biological sample.

Mouse model of CDI

Humanized microbiota mice (^{HMb}mice) were derived from an initial population of germ free C57bl/6 mice stably colonized with human gut microbiota and validated for use as a model of CDI.[28] ^{HMb}mice aged 6-8 weeks of both sexes were treated with a five-antibiotic cocktail consisting of kanamycin (0.4 mg ml^{-1}), gentamicin (0.035 mg ml^{-1}), colistin (850 U ml^{-1}), metronidazole (0.215 mg ml^{-1}), and vancomycin (0.045 mg ml^{-1})) administered *ad libitum* in drinking water for 4 days. Water was switched to antibiotic-free sterile water and 24 hrs later mice were administered an intra-peritoneal (IP) injection of clindamycin (10 mg kg^{-1}). After a further 24 hrs, mice were challenged with 10^4 *C. difficile* spores by oral gavage. Sterile drinking water containing 5 mM trehalose was provided *ad libitum* (for the +/- trehalose study, mice were administered an additional 100 μl oral gavage of 300 mM trehalose daily) and mice were monitored for signs of disease.

In a separate experiment to determine *C. difficile* colonization load and toxin production, mice were euthanized 48 hours following challenge with either R20291 or R20291Δ*treA*. *C. difficile* levels in cecal contents were determined by qPCR of toxin genes.[10] Relative toxin levels were assessed using a Vero Cell rounding assay.[10] Sample sizes for all experiments were determined using power analysis based upon prior experimental data. No randomization of animals was performed; however, all groups were checked to ensure no significant difference in the age, weight or sex of mice between groups prior to starting experiments. All animal use was approved by the Animal Ethics Committee of Baylor College of Medicine (Protocol no. AN-6675).

Detection of trehalose in cecal contents and human ileostomy fluid

Antibiotic treated groups were pre-treated with the 5-antibiotic cocktail for 3 days. Mice were gavaged 100 μl of 5 mM trehalose, 300 mM trehalose or water. Twenty minutes post gavage mice were euthanized, cecal contents harvested and vigorously mixed with 2 volumes/weight ice cold DMM (no carbohydrate). Supernatant was separated by centrifugation, filter sterilized, and reduced in an anaerobic chamber overnight prior to use. Ileostomy effluent from three anonymous donors was self-collected into sterile containers and stored at −20°C until thawed, filter sterilized, and used for assay.

Strains were grown overnight and subcultured 1:50 into DMM supplemented with 20 mM succinate. Upon reaching an OD600 of 0.2-0.3 cells were collected via centrifugation and

resuspended in ~300 μL cecal or ileostomy fluid and incubated anaerobically for 30 minutes. Cells were then centrifuged and resuspended in RNAlater (Invitrogen) prior to qRT-PCR analysis.

Bioreactor model for ribotype 078 Δ*ptsT* competition

Faecal communities were established in continuous-flow minibioreactor arrays as previously described[10] using bioreactor defined medium[29] without starch (BDM4). Communities were disrupted by addition of clindamycin (250 μg ml^{-1}) continuously supplied in the medium for four days. Following clindamycin treatment, communities were supplied BDM4 without clindamycin supplemented with trehalose (5 mM final concentration, $BDM4_{tre}$). After 1 day of growth in $BDM4_{tre}$, to allow washout of clindamycin, communities were challenged with a mixture of exponentially growing CD1015 strains (RT078 wt and Δ*ptsT*). The competitive index (CI) was determined by dividing the proportion of wildtype (wt) cells at the end of the competition by the proportion at the start. The CI of wt:Δ*ptsT* strains was determined by qPCR. The CI of wt vs CD1015ΔptsT::ahTCptsT was calculated by selective plating.

Isolation of spontaneous *treR* mutants

C. difficile strains were inoculated into continuous-flow minibioreactor arrays as previously described[10] using bioreactor defined medium[29] without starch (BDM4) supplemented with 5mM trehalose ($BDM4_{tre}$). Every 24 hours after the start of the experiment 200 μL PBS with containing 100 mM trehalose was spiked into each minibioreactor. The reactors were sampled daily, serially diluted and plated to DMM agar supplemented with 10 mM trehalose. Resulting colonies were streak purified and the ability to grow on low trehalose (10 mM) verified on plates and in broth culture. The *treR* gene was sequenced and compared to the isogenic parent strain.

Statistics

Statistical analyses were performed using R (v. 3.3.2). The Students two sample t-test (2-tailed) was used for comparisons of continuous variables between groups with similar variances; Welch two sample t-test (2-tailed) was used for comparisons of continuous variables between groups with dissimilar variances. P values from multiple comparisons were corrected using the Holm method.[30] Wilcoxon rank sum test with continuity correction was used for the toxin assay where data is non-normal. Fold change data from *treA* gene expression experiments were log-normalized prior to statistical analysis. Data were visualized using individual data points and group means. The cox proportional hazards model and likelihood ratio tests were used to test significant differences in survival distributions among *C. difficile*-challenged groups of animals.

Collection of human bio-specimens

For faecal samples, live subjects who were self-described as healthy and had not consumed antibiotics within the previous two months were recruited to provide faecal samples for human faecal bioreactor experiments. Informed consent was obtained prior to collection of samples and no identifying information was obtained along with the sample. Faecal samples were collected in sterile containers, transported to the laboratory on ice in the presence of

anaerobic gas packs (BD Biosciences) within 16 hrs of collection, manually homogenized in an anaerobic environment, aliquoted into anaerobic tubes, sealed and stored at −80°C until use. Subjects who had ileostomies placed due to a previous, undisclosed illnesses were recruited to provide ileostomy effluents. Informed consent was obtained prior to collection of samples and no identifying information was obtained along with the sample. After transfer from the ostomy bag to a sterile collection container, ileostomy samples were transported to the laboratory on ice within 12 hrs of collection. Upon receipt, samples were stored at −20°C. Ileostomy donors were recruited through the Ostomy Association of Greater Lansing, and were most likely residents of Lansing, Michigan USA and its surrounding counties. Samples were stored at −80°C or −20°C for 3-4 years prior to use. Samples were randomly selected for testing from a bank of available samples. Samples were collected according to a protocol approved by the Institutional Review Board of Michigan State University (Protocol 10-736SM).

Extended Data

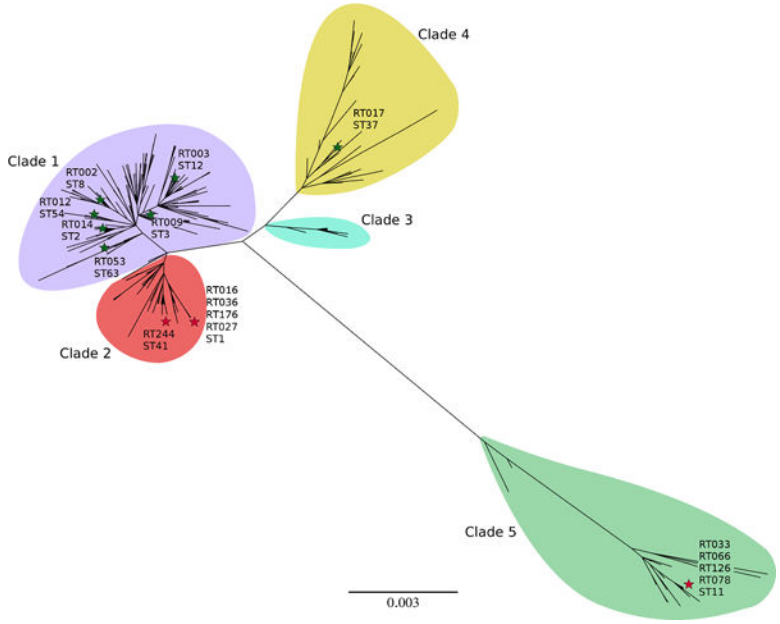

Extended Data Fig. 1.

Phylogenetic organization of C. difficile MLST profiles. Maximum likelihood tree based upon concatenated Multi Locus Sequence Typing genes of the 399 current profiles available at https://pubmlst.org/cdifficile/ .[35] Stars indicate position of strains used in this study with red stars indicating sequence types possessing either the treR L172I (ST1, ST41) or 4 gene insertion (ST11). Tree constructed using MEGA7.[36]

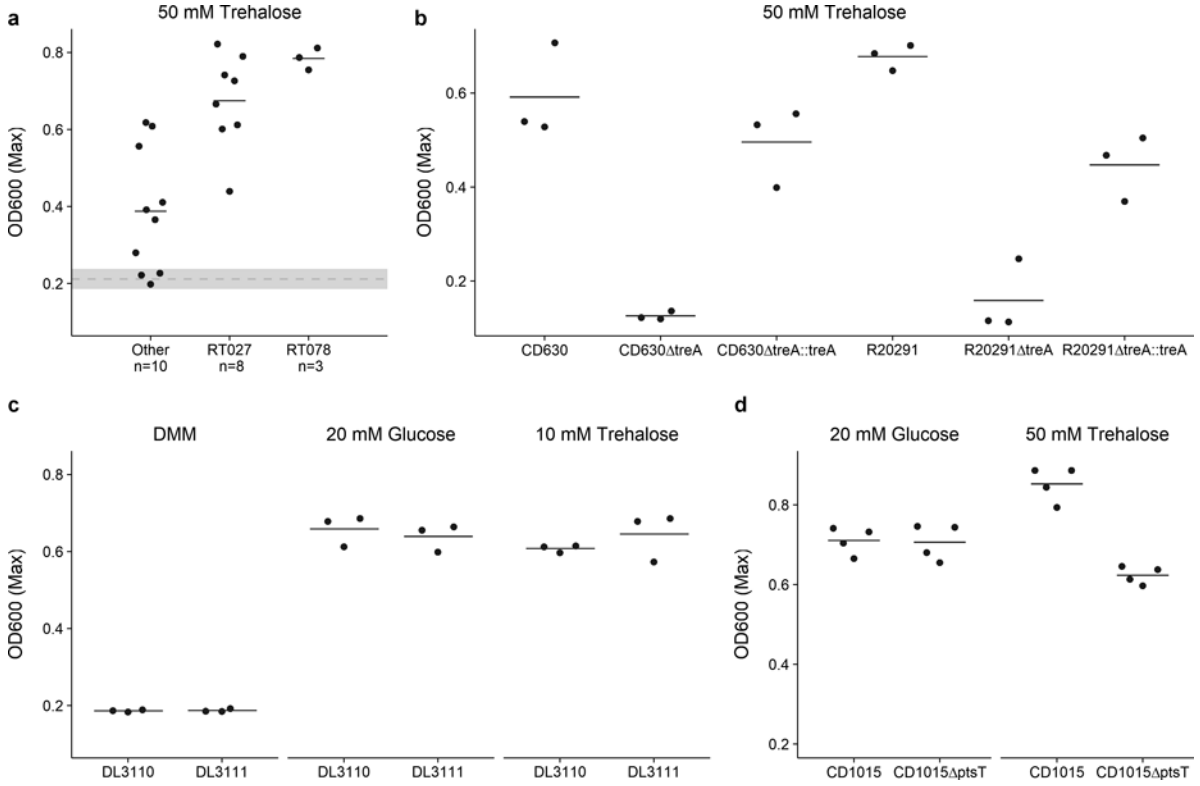

Extended Data Fig. 2. Growth of *C. difficile* strains

a, The majority of strains can grow on 50 mM trehalose. Dashed grey line and band indicate mean growth in DMM without a carbon source and s.d. Solid lines indicate mean growth yield (OD600) for groups: Non-RT027/078 (n=10), RT027 (n=8), and RT078 (n=3). **b**, Deletion of *treA* ablates the ability of both CD630 (RT12) and R20291 (RT027) to grow on trehalose. This phenotype can be restored by supplying *treA* on an inducible plasmid (n=3 for each strain/group). **c**, RT244 strains (DL3110 and DL3111) possessing the treR L172I mutation are capable of growth on 10 mM trehalose (n=3 for each strain/group). **d**, CD1015ΔptsT can metabolize 50 mM trehalose (n=4 for each strain/group). For panels a-d points represent biologically independent samples, solid bars are mean.

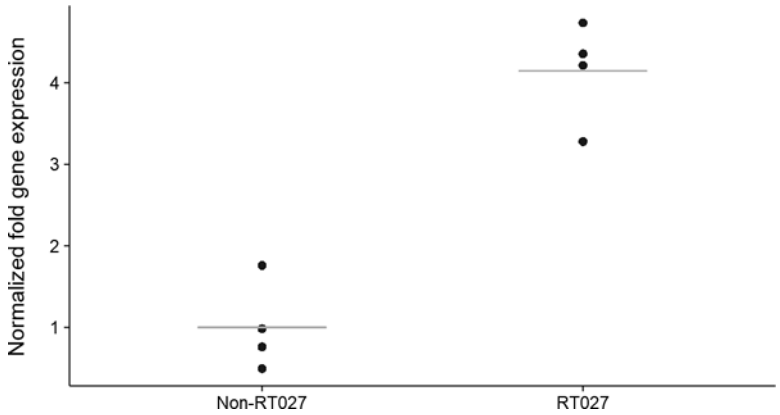

Extended Data Fig. 3. RT027 strains express *treA* at a significantly higher level than non-RT027 strains in the presence of 25 mM trehalose

Each data point (n=4 Ribotypes per group) represents gene expression from a different, biologically independent, strain and is an average from 2-5 independent experiments. P=0.029, Mann-Whitney-Wilcoxon Test (2 sided).

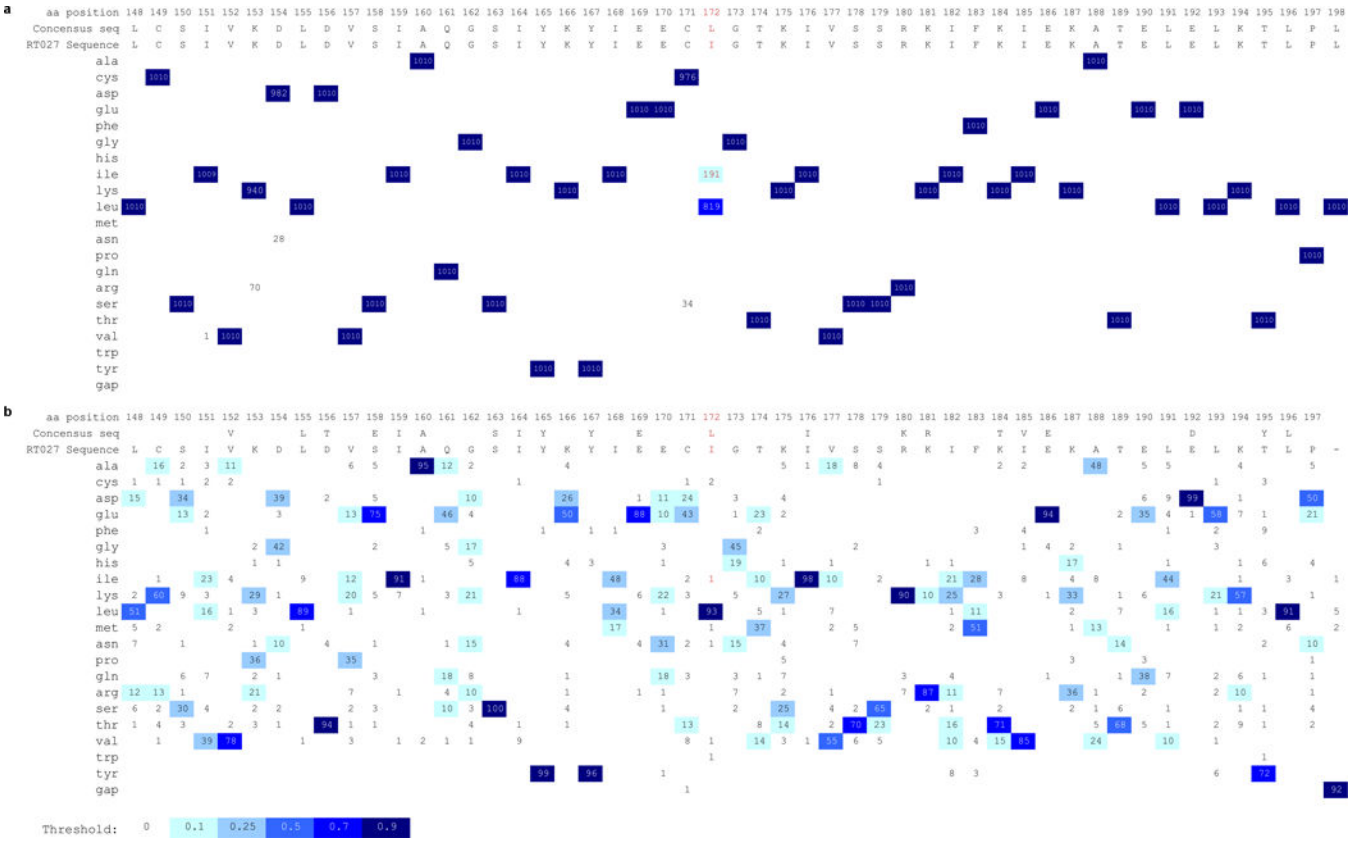

Extended Data Fig. 4. RT027 strains have a L172I mutation at a highly conserved site

a, *treR* genes from available *C. difficile* WGS files on NCBI (accessed 11-May-2017) were identified by tblastn and translated to protein sequences. Sequence fragments < 240 amino acids were discarded and the remaining 1010 sequences aligned with Clustal Omega[37]. All 191 sequences containing the L172I SNP also contained the *thyA* gene, a marker for the RT027 lineage. *ThyA* was not found in any other genomes. Numbers indicate number of sequences with corresponding amino acid in that position. Multiple sequence alignment visualization generated with ProfileGrid.[38] **b**, The TreR protein sequence from RT027 strain R20291 was blasted against non-*C. difficile* sequences in the NCBI database and the top 99 matches (along with $R20291_{treR}$) aligned with Clustal Omega. The Leucine at position 172 was found to be conserved in 93 of 99 non-C. *difficile* sequences. To confirm the importance of this residue, TreR was blasted against all non-Clostridial sequences in the NCBI database and the top 500 hits saved. Following removal of duplicate species 191 sequences were aligned with Clustal Omega. The Leucine at residue 172 was conserved in 83% of sequences (not shown).

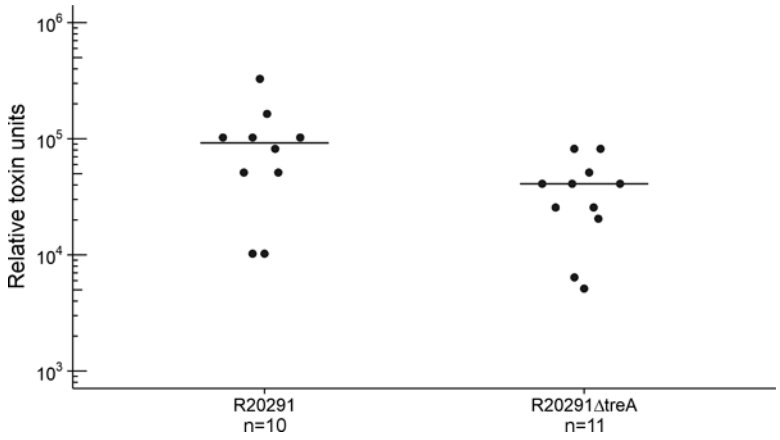

Extended Data Fig. 5. A *treA* knockout strain has decreased toxin production 48 hours after infection

Mice were gavaged 10^4 spores of either R20291 or R20291Δt*reA* and provided 5 mM trehalose in drinking water. Points represent toxin levels from individual mice (R20291 n=10, R20291Δt*reA* n=11) euthanized 48 hours after infection. Bars are mean. Mice gavaged with R20291Δt*reA* had significantly lower toxin levels (p=.0268 Wilcoxon-Mann-Whitney test (2 sided), median 40960, IQR 23040-46080 Vs 92160, IQR 51200-102400).

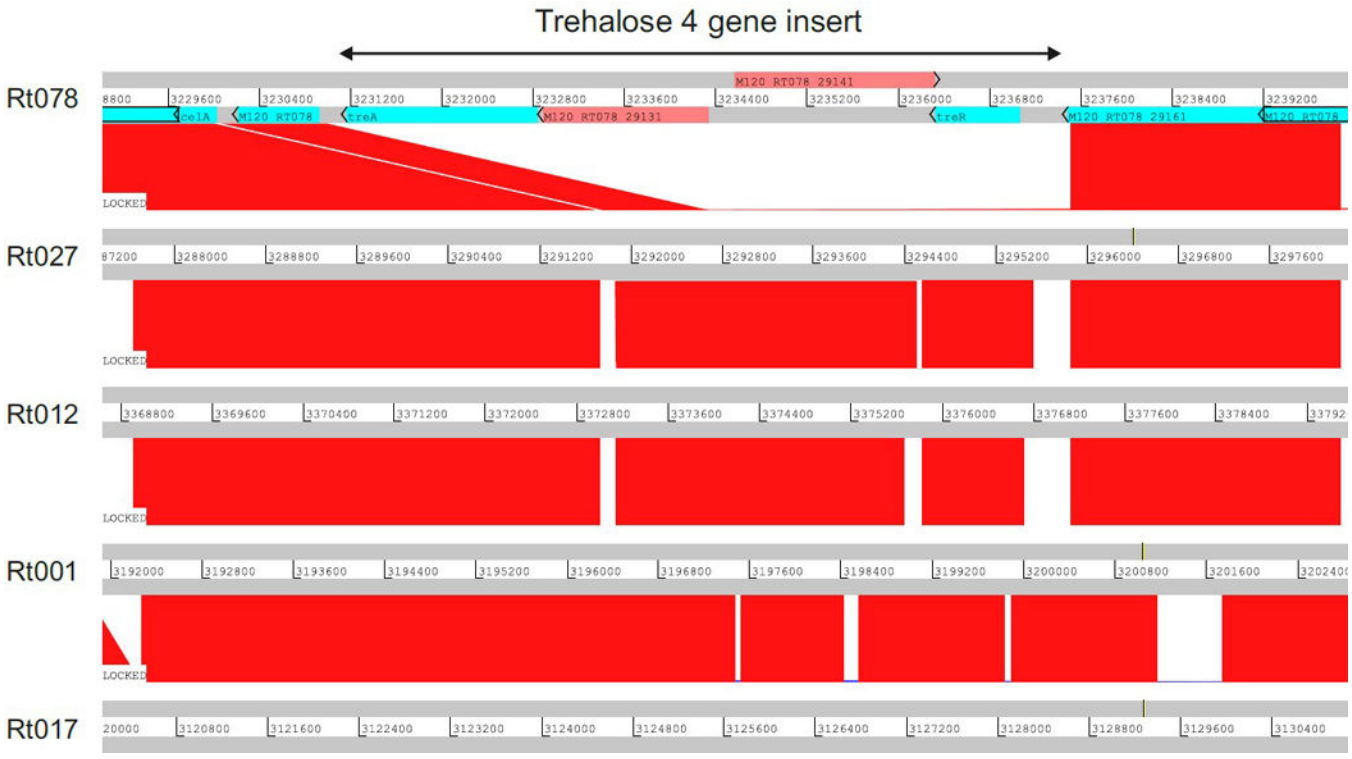

Extended Data Fig. 6. The 4 gene trehalose insertion is only present in the RT078 lineage

Artemis comparison tool (ACT) displaying pairwise comparisons between *C. difficile* RT078 genome (M120) sequence and genome sequences from other *C. difficile* ribotypes (ribotypes indicated on the left). Numbers between grey bars indicate the genomic region

where the trehalose four gene insert is located (3231169..3237057). Regions of sequence homology are displayed in red. The trehalose four gene insert of RT078 (indicated by the arrow on the top) was observed in RT078, but absent in other ribotypes.

Extended Data Table 1

Compounds conferring ≥ 1.5-fold growth advantage in Biolog Phenotypic Microarray plates PM1 or PM2.

	Compound	CD630	CD2015
PM1:	N-acetyl-D-glucosamine	+	+
	L-proline	−	−
	D-trehalose	+	+
	D-mannose	+	+
	D-sorbitol	−	+
	D-mannitol	+	+
	D-fructose	−	+
	α-D-glucose	+	+
	α-Keto-Butyric acid	+	−
	L-serine	+	−
	L-threonine	−	−
	glycyl-L-proline	−	−
PM2:	N-acetyl-neuraminic acid	+	+
	D-arabitol	−	+
	arbutin	+	+
	D-melezilose	+	+
	salicin	+	+
	D-tagatose	+	+
	D-glucosamine	+	+
	β-hydroxy-butyric acid	+	+
	α-keto valeric acid	+	+
	hydroxy-L-proline	−	+
	L-leucine	+	+
	L-methionine	−	+

Results of individual experiment where growth was (+) or was not (−) increased by at least 1.5-fold over DMM control.

Extended Data Table 2

Spontaneous *C. difficile* mutants able to utilize 10 mM trehalose.

Strain	Ribotype	Nonsense mutation*	Missense mutation	Insertions/deletions	Number of independent isolates
3014	001	18	–	–	1
2012	002	63	–	–	1
2012	002	89	–	–	2
2012	002	15	–	–	1
2012	002	22	–	–	1

Strain	Ribotype	Nonsense mutation*	Missense mutation	Insertions/deletions	Number of independent isolates
2012	002	–	S20I	–	1
2012	002	64	–	–	1
2012	002	24	–	–	1
2012	002	20	–	–	1
1014	014	–	S41I, T118K	1	1
1014	014	–	T118K	–	1
2048	053	70	–	–	1

*Numbers refer to the position in the consensus TreR amino acid sequence which become a premature stop codon.

Extended Data Table 3

Strains, Primers, and Plasmids.

Strains	Ribotype	MLST (Clade)	Note	Reference
CD630	12	54 (1)	Erythromycin sensitive	[31]
CD630Δ*treA*	12	54 (1)		This Study
CD630 pRFP185-P_{aTc}-*ptsT*	12	54 (1)		This Study
CD630Δ*treA* pRFP185-P_{aTc}-*treA*	12	54 (1)		This Study
R20291	27	1 (2)		[24]
R20291Δ*pyrE*	27	1 (2)		[24]
R20291Δ*treA*	27	1 (2)		This Study
R20291Δ*treA* pRFP185-P_{aTC}-*treA*	27	1 (2)		This Study
CD1015	78	11 (5)		†
CD1015Δ*pyrE*	78	11 (5)		This Study
CD1015Δ*ptsT*	78	11 (5)		This Study
CD1015Δ*ptsT* pRFP185-P_{aTc}-*ptsT*	78	11 (5)		This Study
VPI10463	3	12(1)	High toxin producer	
CD196	27	1 (2)	Ancestral RT027 strain	[32]
CD1007	053-163	63 (1)		†
CD1014	014-20	2 (1)		[10]
CD2012	2	8 (1)		†
CD2018	unique UM isolate			†
CD2046	unique UM isolate			†
CD2048	053-163	63 (1)		[10]
CD37	9	3 (1)	Non-toxigenic strain	[33]
CD4004	2	8 (1)		†
CD4011	1	3 (1)		†
CD2015	27	1 (2)		[10]
CD3017	27	1 (2)		[10]
CD4010	27	1 (2)		[10]
CD4012	27	1 (2)		†
CD4015	27	1 (2)		[10]
CD2001	78	11 (5)		†

Strains	Ribotype	MLST (Clade)	Note	Reference
CD2058	78	11 (5)		†
DL3110	244	41 (2)	contains L172I in treR	[11]
DL3111	244	41 (2)	contains L172I in treR	[11]

Primers	Note		Sequence 5′ – 3′
IBS1.2	Insertional deletion of *treA* in CD630		atatcaagcttttgcaacccacgtcgatcgtgaatagaagattattgtgcgcccagatagggtg
EBS1			cagattgtacaaatgtggtgataacagataagtcattattattaacttacctttctttgt
EBS2			cgcaagtttctaatttcggttttctatcgatagaggaaagtgtct
CR064	CD630 *treA* insertion check		gcaacaatgatggtataggtgatataaatgg
CR065			ggaacagaaccatcaggtttagca
JCb092	Upstream homology arm R20291 *treA*	5′ phosphorylated	agacctttaaggagggataggggt
JCb093		5′ phosphorylated	aggagaaacgtacataggagtcaacca
JCb094	Downstream homology arm R20291 *treA*	5′ phosphorylated	cctgaaacttatttgaataaattaaactacac
JCb095		5′ phosphorylated	gtttgatactgatggagggcctta
JCb096			gccctccatcagtatcaaacggggatcctctagagtcgac
JCb097	Bridging oligos for ligase cycling		ctcctatgtacgtttctcctcctgaaacttatttgaataa
JCb098			cgaattcgagctcggtacccagacctttaaggagggatag
JCb135	Upstream homology arm CD1015 *pyrE*	*SbfI*	atacctgcaggagggacatttttattatcttcag
JCb136		5′ phosphorylated	acaacatcttcagcaattattatctttg
JCb137	Spacer from pMTL-YN2	5′ phosphorylated	gcggccgctgtatccatatgacc
JCb138		5′ phosphorylated	actagcgccattcgccattcagg
JCb139	Downstream homology arm CD1015 *pyrE*	5′ phosphorylated	gcggccgctgtatccatatgacc
JCb140		*AscI*	atatggcgccgccataacattaataaaatttaaaatcaataattat
JCb141	Bridging oligos for ligase cycling		ataattgctgaagatgttgtgcggccgctgtatccatatg
JCb142			gaatggcgaatggcgctagttaataaaaacttaattattt
JCb153	Upstream homology arm CD1015 *ptsT*	*EcoRI*	atagaattcaaaaacccaaaaatttaacc
JCb154		*BamHI*	ataggatccatctacttatcctttctctttttattataag
JCb155	Downstream homology arm CD1015 *ptsT*	*BamHI*	ataggatcccaaatgacaatatataaatataattcccttgg
JCb156		*NcoI*	ataccatggcgtggttggtcatggttaca
JCb167	CD1015Δ*ptsT* check		cggaatttcttttatattcatttgg
JCb168			cccaatttgttggagcactt
JCb225	Conformation of *pyrE* knockout/repair		atgggaatgggcggaataac
JCb226			gcttggaagcagctacaacaga
JCb211	CD1015 *pyrE* repair	*NotI*	atagcggccgcttacattcctaattccttgaactctc
JP048	qPCR for C. *difficile* 16S DNA		ttgagcgatttacttcggtaaaga
JP049			ccatcctgtactggctcacct
CR045	qPCR for C. *difficile* *treA* DNA		tacgctgatggtcctcgtat
CR046			cgcctcctttataatctgttttc

Plasmids	Reference
pMTL-YN2	[24]
pMTL-YN2C	[24]

Plasmids	Reference
pMTL-YN4	[24]
pRPF185	[34]
Plasmid Maps	
pJC-R20291*treA*KO	https://benchling.com/s/seq-DANCiRRu7FwNqRJC09iu
pJC-CD1015*pyrE*KO	https://benchling.com/s/seq-Km3QbgAkU66DkNtaOA4R
pRFP185-P_{aTc}-*ptsT*	https://benchling.com/s/seq-hKTbvE2pfE8MpvvEqFce
pJC-CD1015*pyrE*Repair	https://benchling.com/s/seq-d25nmFmvSPtR1iQB8vka
pRFP185-P_{aTc}-*treA*	https://benchling.com/s/seq-TTthHzlU2fsfRZ94oD9V

†Clinical isolates obtained from the Michigan Department of Community Health (MDCH). Collected from Michigan hospitals between December 2007 and May 2008 References

Acknowledgments

This work was supported by the NIH (U01AI124290-01 & 5U19AI09087202). The authors thank the members of the Ostomy Association of Greater Lansing for anonymously donating samples and Dr. Dena Lyras for the RT244 strains. We thank Vincent Young, David Mills, Jens Walter and Mauro Costa-Mattioli for comments on the manuscript.

References

1. He M, et al. Emergence and global spread of epidemic healthcare-associated Clostridium difficile. Nat Genet. 2012; :1–6. DOI: 10.1038/ng.2478
2. Spigaglia P, et al. Fluoroquinolone resistance in Clostridium difficile isolates from a prospective study of C. difficile infections in Europe. J Med Microbiol. 2008; 57:784–789. [PubMed: 18480338]
3. Spigaglia P, Barbanti F, Dionisi AM, Mastrantonio P. Clostridium difficile isolates resistant to fluoroquinolones in Italy: Emergence of PCR ribotype 018. J Clin Microbiol. 2010; 48:2892–2896. [PubMed: 20554809]
4. Jhung MA, et al. Toxinotype V Clostridium difficile in humans and food animals. Emerg Infect Dis. 2008; 14:1039–1045. [PubMed: 18598622]
5. Goorhuis A, et al. Emergence of Clostridium difficile infection due to a new hypervirulent strain, polymerase chain reaction ribotype 078. Clin Infect Dis. 2008; 47:1162–1170. [PubMed: 18808358]
6. Khanna S, Gupta A. Community-acquired Clostridium difficile infection: an increasing public health threat. Infect Drug Resist. 2014; 7:63. [PubMed: 24669194]
7. Limbago BM, et al. Clostridium difficile strains from community-associated infections. J Clin Microbiol. 2009; 47:3004–7. [PubMed: 19571021]
8. Walker AS, et al. Relationship between bacterial strain type, host biomarkers, and mortality in clostridium difficile infection. Clin Infect Dis. 2013; 56:1589–1600. [PubMed: 23463640]
9. He M, et al. Evolutionary dynamics of Clostridium difficile over short and long time scales. Proc Natl Acad Sci U S A. 2010; 107:7527–32. [PubMed: 20368420]
10. Robinson CD, Auchtung JM, Collins J, Britton RA. Epidemic Clostridium difficile strains demonstrate increased competitive fitness compared to nonepidemic isolates. Infect Immun. 2014; 82:2815–2825. [PubMed: 24733099]
11. Lim SK, et al. Emergence of a ribotype 244 strain of clostridium difficile associated with severe disease and related to the epidemic ribotype 027 strain. Clin Infect Dis. 2014; 58:1723–1730. [PubMed: 24704722]
12. Eyre DW, et al. Emergence and spread of predominantly community- onset Clostridium difficile PCR ribotype 244 infection in Australia, 2010 to 2012. 2015:1–10.
13. Polivkova S, Krutova M, Petrlova K, Benes J, Nyc O. Clostridium difficile ribotype 176 - A predictor for high mortality and risk of nosocomial spread? Anaerobe. 2016; 40:35–40. [PubMed: 27155489]

14. Rupnik M, et al. Distribution of Clostridium difficile PCR ribotypes and high proportion of 027 and 176 in some hospitals in four South Eastern European countries. Anaerobe. 2016; doi: 10.1016/j.anaerobe.2016.10.005
15. Bergoz R. Trehalose malabsorption causing intolerance to mushrooms. Report of a probable case. Gastroenterology. 1971:909–12. [PubMed: 5104075]
16. Bergoz R, Bolte JP, Meyer zum Bueschenfelde. Trehalose tolerance test. Its value as a test for malabsorption. Scand J Gastroenterol. 1973; 8:657–63. [PubMed: 4129178]
17. Oku T, Nakamura S. Estimation of intestinal trehalase activity from a laxative threshold of trehalose and lactulose on healthy female subjects. Eur J Clin Nutr. 2000; 54:783–788. [PubMed: 11083487]
18. Higashiyama T. Novel functions and applications of trehalose. Pure Appl Chem. 2002; 74:1263–1269.
19. Stabler RA, et al. Comparative genome and phenotypic analysis of Clostridium difficile 027 strains provides insight into the evolution of a hypervirulent bacterium. Genome Biol. 2009; 10:R102. [PubMed: 19781061]
20. Leffler DA, Lamont JT. Clostridium difficile Infection. N Engl J Med. 2015; 372:1539–1548. [PubMed: 25875259]
21. Theriot CM, et al. Antibiotic-induced shifts in the mouse gut microbiome and metabolome increase susceptibility to Clostridium difficile infection. Nat Commun. 2014; 5
22. Knetsch CW, et al. Genetic markers for Clostridium difficile lineages linked to hypervirulence. Microbiology. 2011; 157:3113–3123. [PubMed: 21873406]
23. Bouillaut L, Self WT, Sonenshein AL. Proline-dependent regulation of Clostridium difficile stickland metabolism. J Bacteriol. 2013; 195:844–854. [PubMed: 23222730]
24. Ng YK, et al. Expanding the repertoire of gene tools for precise manipulation of the Clostridium difficile genome: allelic exchange using pyrE alleles. PLoS One. 2013; 8:e56051. [PubMed: 23405251]
25. Fagan RP, Fairweather NF. Clostridium difficile has two parallel and essential Sec secretion systems. J Biol Chem. 2011; 286:27483–93. [PubMed: 21659510]
26. De Kok S, et al. Rapid and Reliable DNA Assembly via Ligase Cycling Reaction. 2014
27. Pfaffl MW. Relative quantification. Real-time PCR. 2006:63–82.
28. Collins J, Auchtung JM, Schaefer L, Eaton KA, Britton Ra. Humanized microbiota mice as a model of recurrent Clostridium difficile disease. Microbiome. 2015; 3:35. [PubMed: 26289776]
29. Auchtung, JM., Robinson, CD., Farrell, K., Britton, RA. Clostridium difficile: Methods and Protocols. Roberts, AP., Mullany, P., editors. Springer; New York: 2016. p. 235-258.
30. Holm S. A simple sequentially rejective multiple test procedure. Scand J Stat. 1979; 6:65–70.
31. Dingle TC, Mulvey GL, Armstrong GD. Mutagenic analysis of the clostridium difficile flagellar proteins, flic and flid, and their contribution to virulence in hamsters. Infect Immun. 2011; 79:4061–4067. [PubMed: 21788384]
32. Popoff MR, Rubin EJ, Gill DM, Boquet P. Actin-specific ADP-ribosyltransferase produced by a Clostridium difficile strain. Infect Immun. 1988; 56:2299–2306. [PubMed: 3137166]
33. Smith CJ, Markowitz SM, Macrina FL. Transferable tetracycline resistance in Clostridium difficile. Antimicrob Agents Chemother. 1981; 19:997–1003. [PubMed: 7271279]
34. Fagan RP, Fairweather NF. Clostridium difficile has two parallel and essential Sec secretion systems. J Biol Chem. 2011; 286:27483–93. [PubMed: 21659510]
35. Griffiths D, et al. Multilocus sequence typing of Clostridium difficile. J Clin Microbiol. 2010; 48:770–778. [PubMed: 20042623]
36. Kumar S, Stecher G, Tamura K. MEGA7: Molecular Evolutionary Genetics Analysis Version 7.0 for Bigger Datasets. Mol Biol Evol. 2016; 33:1870–1874. [PubMed: 27004904]
37. Sievers F, et al. Fast, scalable generation of high-quality protein multiple sequence alignments using Clustal Omega. Mol Syst Biol. 2011; 7:539. [PubMed: 21988835]
38. Roca AI, Abajian AC, Vigerust DJ. ProfileGrids solve the large alignment visualization problem: influenza hemagglutinin example. F1000Research. 2013; doi: 10.3410/f1000research.2-2.v1

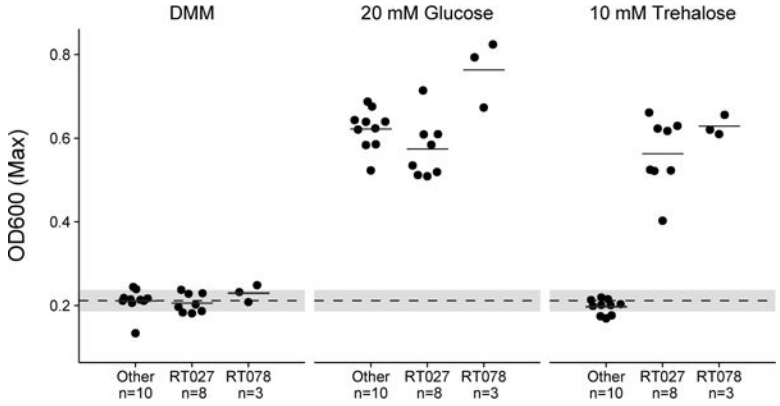

Figure 1. Only RT027 and 078 strains show enhanced growth on 10 mM trehalose

Dashed grey line and band indicate mean growth in DMM without a carbon source and s.d. for all samples (n=21). Solid lines are mean growth yield (OD600) for groups: Non-RT027/078 (n=10), RT027 (n=8), and RT078 (n=3). All points represent biologically independent samples.

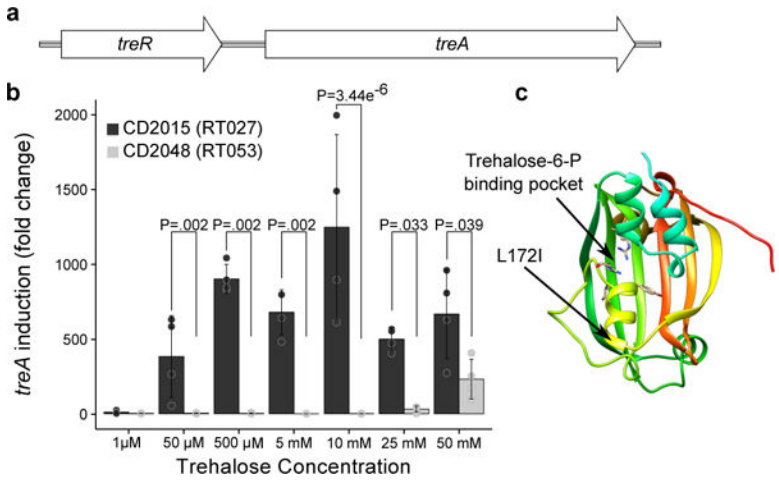

Figure 2. *treA* is responsible for trehalose metabolism

a, Trehalose metabolism operon found in all *C. difficile* strains; consisting of a phosphotrehalase (*treA*) and its transcriptional regulator (*treR*). **b**, RT027 strains strongly induce *treA* at 50 μM trehalose and at a significantly higher level than non-RT027 strains (n=4 biologically independent samples per trehalose concentration/strain). Bars are average fold increase, error bars are s.d.; p values derived from t-test (2-tailed) and Holm corrected for multiple comparisons. **c**, Structure of TreR monomer highlighting proximity of L172I mutation to trehalose-6-P binding pocket.

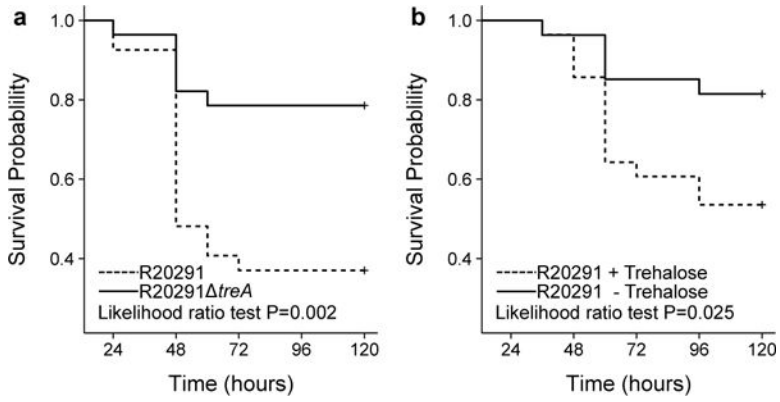

Figure 3. Trehalose metabolism increases virulence

a, Mice Infected with R20291Δ*treA* (n=27 animals) have significantly attenuated risk of mortality when compared to mice infected with R20291 (n=28 animals) (78% lower risk with Δ*treA* mutant; hazard ratio, 0.22; 95% CI, 0.09 to 0.59; P=0.003). **b**, Mice infected with R20291 (RT027) have a significantly higher risk of mortality when trehalose is supplemented in the diet (n=28 animals) than those with no trehalose supplementation (n=27 animals) (3-fold increased risk with trehalose; hazard ratio, 3.20; 95% CI, 1.09 to 9.42; P=0.035). All statistical tests were 2 sided.

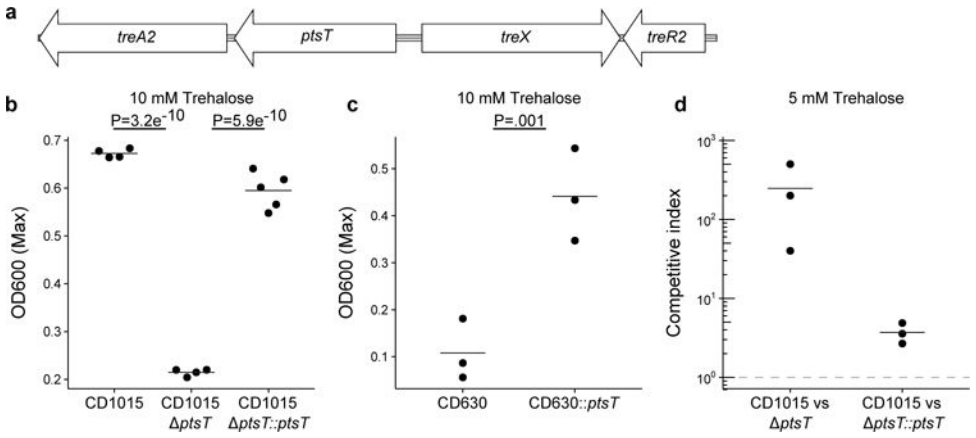

Figure 4. *ptsT* enables enhanced trehalose metabolism

a, Structure of horizontally acquired trehalose metabolism module found in RT078 and closely related strains. **b**, Deletion of the trehalose transporter from a clinical RT078 strain (CD1015) ablates its ability to grow on 10 mM trehalose. Expression of *ptsT* from an inducible plasmid restores growth of CD1015ΔptsT on 10 mM trehalose, (CD1015, n=4; CD1015Δ*ptsT*, n=4; CD1015Δ*ptsT::ptsT*, n=5). **c**, Expressing *ptsT* from an inducible plasmid enables enhanced growth of CD630 (RT012) on 10 mM trehalose (CD630 n=3; CD630*::ptsT* n=3). **d**, The *ptsT* provides a competitive advantage in complex microbial communities. Dashed grey line (CI = 1) indicates equal fitness of the competing strains, points above this line represent out-competition by CD1015. All points (Fig 4b-d) represent biologically independent samples, bars are mean, p values derived from t-test (2-tailed) and Holm corrected for multiple comparisons where appropriate.

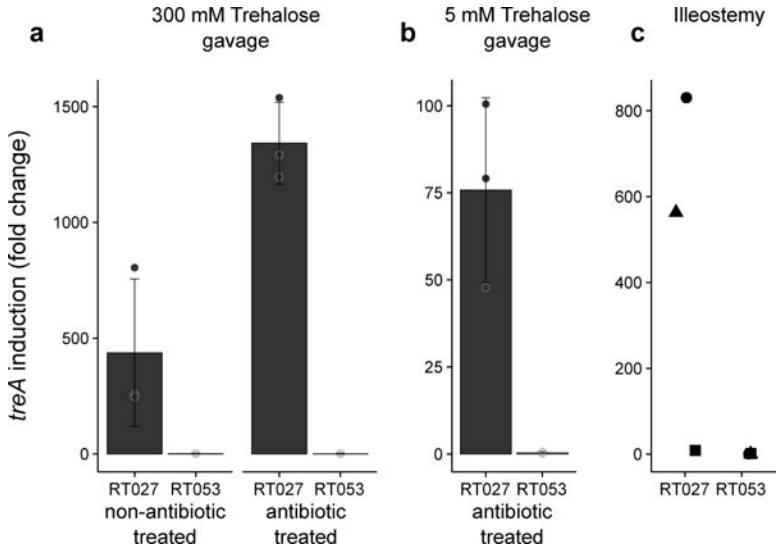

Figure 5. Trehalose can be detected in murine cecum and human ileostomy fluid

a, Twenty minutes post gavage, trehalose reaches high enough levels in the murine cecum to turn on expression of *treA* in RT027 but not non-RT027 in both non-antibiotic and antibiotic treated mice (n=3 animals per trehalose concentration/strain). **b**, trehalose can be detected by RT027 but not non-RT027 in the cecum of antibiotic treated mice gavaged with just 100 μl 5 mM trehalose (n=3 animals per group). **c**, RT027 strains can detect trehalose in 2/3 human ileostomy fluid samples tested from patients eating a normal (no deliberate trehalose addition) diet. Points represent biologically independent replicates, bars are average fold increase, error bars are s.d.

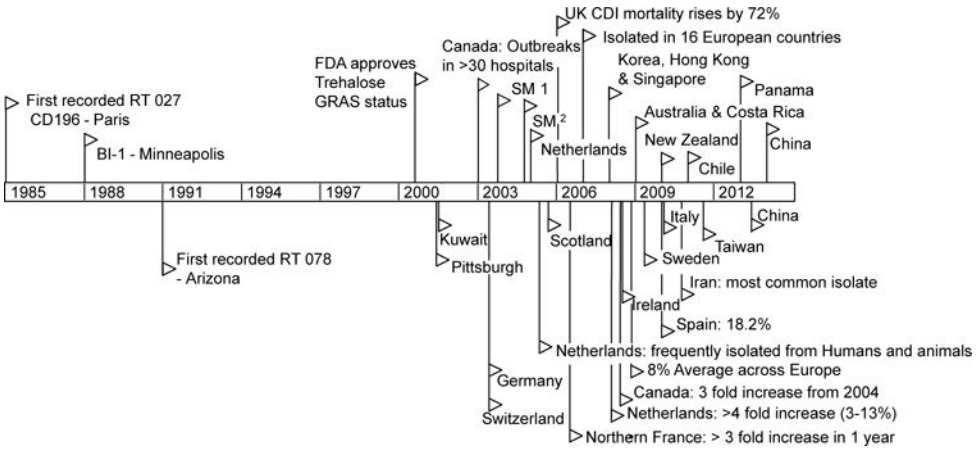

Figure 6. Timeline of trehalose adoption and spread of RT027 & RT078 lineages

Flags indicate reported outbreaks or first reports of ribotype 027 (top) or 078 (bottom) in PubMed. † Stoke Mandeville outbreaks.